Contents lists available at ScienceDirect

International Journal of Pharmaceutics

pH-sensitive niosomes for ATRA delivery: A promising approach to inhibit Pin1 in high-grade serous ovarian cancer

Maria Valeria Giuli [a,1], Patrizia Nadia Hanieh [b,1], Jacopo Forte [b], Maria Gioia Fabiano [b], Angelica Mancusi [c], Bianca Natiello [c], Federica Rinaldi [b,*], Elena Del Favero [d], Maria Grazia Ammendolia [e], Carlotta Marianecci [b], Saula Checquolo [a,2], Maria Carafa [b,2]

[a] *Department of Medico-Surgical Sciences and Biotechnology, Sapienza University of Rome, Laboratory affiliated to Istituto Pasteur Italia-Fondazione Cenci Bolognetti, Corso della Repubblica 79, 04100 Latina, Italy*
[b] *Department of Drug Chemistry and Technology, Sapienza University of Rome, Piazzale Aldo Moro 5, 00185 Rome, Italy*
[c] *Department of Molecular Medicine, Sapienza University of Rome, Viale Regina Elena 291, 00161 Rome, Italy*
[d] *Department of Medical Biotechnologies and Translational Medicine, University of Milan, Via Fratelli Cervi 93, 20090, Segrate, Italy*
[e] *National Center for Innovative Technologies in Public Health, Istituto Superiore di Sanità, Viale Regina Elena 299, 00161 Rome, Italy*

A R T I C L E   I N F O

A B S T R A C T

The peptidyl-prolyl *cis/trans* isomerase Pin1 positively regulates numerous cancer-driving pathways, and it is overexpressed in several malignancies, including high-grade serous ovarian cancer (HGSOC). The findings that all-trans retinoic acid (ATRA) induces Pin1 degradation strongly support that ATRA treatment might be a promising approach for HGSOC targeted therapy. Nevertheless, repurposing ATRA into the clinics for the treatment of solid tumors remains an unmet need mainly due to the insurgence of resistance and its ineffective delivery. In the present study, niosomes have been employed for improving ATRA delivery in HGSOC cell lines. Characterization of niosomes including hydrodynamic diameter, ζ-potential, morphology, entrapment efficiency and stability over time and in culture media was performed. Furthermore, pH-sensitiveness and ATRA release profile were investigated to demonstrate the capability of these vesicles to release ATRA in a stimuli-responsive manner. Obtained results documented a nanometric and monodispersed samples with negative ζ-potential. ATRA was efficiently entrapped, and a substantial release was observed in the presence of acidic pH (pH 5.5). Finally, unloaded niosomes showed good biocompatibility while ATRA-loaded niosomes significantly increased ATRA Pin1 inhibitory activity, which was consistent with cell growth inhibition. Taken together, ATRA-loaded niosomes might represent an appealing therapeutic strategy for HGSOC therapy.

1. Introduction

High-grade serous ovarian cancer (HGSOC) is the commonest subtype of epithelial ovarian cancer (EOC). EOC accounts for 90 % of ovarian tumors and it is one of the most lethal gynecological malignancies due to its insidious nature and the ineffectiveness of the screening tests (Kurnit et al., 2021). Indeed, it is mostly occult at the onset and, when diagnosed, it has already invaded the peritoneum and the organs located in the abdominal cavity (Torre et al., 2018). Furthermore, it is highly heterogeneous, and it yields different clinical outcomes in individual patients (Song et al., 2022). Currently, HGSOC standard treatment includes debulking surgery followed by platinum-based chemotherapy (Kuroki and Guntupalli, 2020). Nevertheless, most patients relapse within two years and the prognosis remains poor (Beesley et al., 2014), thereby underpinning that developing more effective treatments is an unmet need.

---

* Corresponding author.
E-mail addresses: mariavaleria.giuli@uniroma1.it (M.V. Giuli), patrizianadia.hanieh@uniroma1.it (P.N. Hanieh), jacopo.forte@uniroma1.it (J. Forte), mariagioia. fabiano@uniroma1.it (M.G. Fabiano), angelica.mancusi@uniroma1.it (A. Mancusi), bianca.natiello@uniroma1.it (B. Natiello), federica.rinaldi@uniroma1.it (F. Rinaldi), elena.delfavero@unimi.it (E. Del Favero), maria.ammendolia@iss.it (M.G. Ammendolia), carlotta.marianecci@uniroma1.it (C. Marianecci), saula. checquolo@uniroma1.it (S. Checquolo), maria.carafa@uniroma1.it (M. Carafa).
[1] These authors equally contributed to the work.
[2] These authors share the senior authorship.

At this purpose, one appealing candidate might be the peptidyl-prolyl *cis/trans* isomerase Pin1. Indeed, an increasing number of studies has shown that Pin1 plays a pivotal role in several aspects of cancer development and progression (Franciosa et al., 2016; Lu and Hunter, 2014; Yu et al., 2020; Zhou and Lu, 2016). Furthermore, Pin1 is overexpressed in several cancers (Bao et al., 2004), including ovarian cancer (Spena et al., 2018). Finally, Pin1-null mice develop normally (Liou et al., 2002), thereby highlighting that Pin1 inhibition should aid in cancer therapy without causing general side effects on normal tissues.

Collectively, these findings support that Pin1 might be considered an intriguing target for HGSOC cancer therapy.

All-*trans* retinoic acid (ATRA) inhibits and degrades Pin1 by directly binding to the substrate phosphate- and proline-binding pockets in the Pin1 active site (Wei et al., 2015). Clinically, the use of ATRA in combination with other chemotherapeutic drugs represents the suitable therapeutic approach for the treatment of acute promyelocytic leukemia in adults and neuroblastoma in children (Masetti et al., 2012).

Nevertheless, repurposing ATRA for solid tumors remains a daunting task for several reasons: 1. 'acute retinoid resistance' in patients (Chlapek et al., 2018); 2. low aqueous solubility (Szuts and Harosi, 1991), which does not allow its parenteral administration; 3. susceptibility to light, heat and oxidants; and 4. reduced half-life in plasma due to its metabolism regulation by CYP-450 in the liver (Muindi et al., 1992).

Over the years, a wide range of studies have been performed to enhance the benefit of this molecule, mainly focusing on overcoming ATRA resistance, or improving its delivery by employing drug-carriers (Giuli et al., 2020b). This innovative approach has also allowed to overcome the several limitations associated with the current drug therapy such as toxicity and non-targeting. In this scenario, Aronex Pharmaceuticals have manufactured the ATRAGEN™, all-trans-retinoic acid-loaded liposomes, which is the unique ATRA based formulation tested in clinical trials (Ozpolat et al., 2003). Despite FDA approval failure, the promising results on cancer prompted further investigations to identify novel and smart delivery and targeting strategies (Asadipour et al., 2023).

Over the past two decades, niosomes (Nio) have been proposed as carriers for several drugs, e.g. anticancer (Amale et al., 2021; Pourmoghadasiyan et al., 2022), anti-inflammatory, antibacterial and anti-biofilm (Haddadian et al., 2022; Piri-Gharaghie et al., 2022; Shadvar et al., 2021), antifungal, and also as tumor targeting and diagnostic imaging agents (Mirzaei-Parsa et al., 2020).

Like liposomes, Nio are non-immunogenic, biocompatible and biodegradable vehicles, and are capable to deliver drugs into the bilayers' domain, including both hydrophilic, inner aqueous core, and hydrophobic molecules (Marianecci et al., 2014), in a controlled and/or sustained manner at a target site. Moreover, the incorporation of drugs in nanosized carriers not only allows the decrease of systemic toxicity, due to their decreased volume distribution (Barenholz, 2012), but also enables the drug protection from the biological environment, thereby promoting its blood circulation. These nanocarriers are arranged by hydrated self-assembly of non-ionic surfactants, like sorbitan esters and polysorbates, widely used as emulsifiers and stabilisers in several pharmaceutical formulations, food, and cosmetic products, in combination with cholesterol (Chol) which improves niosomal bilayer rigidity, making them very stable compared to other vesicular carriers (Schoellhammer et al., 2014).

In recent years, Nio provided an alternative to liposomes for pharmaceutical delivery due to several advantages such as high chemical stability, high reproducible production, and low manufacturing cost (Kazi et al., 2010). Furthermore, the versatility of their structure promotes their easy design for a wide range of applications. Indeed, depending on the type of surfactant used, the selected drug, the type of disease, and the targeted body site, niosomal surface can be tailored to answer to specific stimuli (internal or external) such as acidic pH (Yasamineh et al., 2022). Noteworthy, drug delivery systems that respond to a change in pH can escape the endosome, where the pH falls

to around 5.5 (Bareford and Swaan, 2007), and favour cytosolic delivery.

Taken together, to obtain an efficient ATRA delivery, we used previously developed empty niosomes, composed by two different surfactants (Tween 20 and Tween 21), named NT20 and NT21, that have been loaded with ATRA and deeply characterised (Carafa et al., 2009; Di Marzio et al., 2008; Di Marzio et al., 2011; Rinaldi et al., 2022).

The main aim of this study is to evaluate the effects of ATRA delivered by niosomes *versus* free ATRA in different ovarian cancer cells, focusing on its known inhibitory impact on Pin1 protein levels, with the ambitious goal of developing a novel smart delivery system to ameliorate the current treatments of HGSOC-bearing patients.

2. Material and methods

2.1. Materials

Polysorbate 20 (Tween 20, Tw20), cholesterol (Chol), all-trans retinoic acid (ATRA), 8-hydroxypyrene-1,3,6-trisulfonic acid trisodium salt (HTPS), pyrene (Pyr), human serum (HS), Hepes salt (N-(2-Hydroxyethyl)piperazine-N′-(2-ethanesulfonic acid) sodium salt), calcein, sodium acetate, acetic acid glacial, Sephadex G-75, were purchased from Sigma-Aldrich (Milan, Italy). Tween 21 (Tw21) was gently gifted from Croda Italiana S.p.a (Mortara Pavia, Italy). Dialysis membranes (MWCO 8000 Da), ethanol, methanol and chloroform were provided from Carlo Erba Reagents Srl (Cornaredo, Milan, Italy). All other products and reagents were of analytical grade.

2.2. Vesicle preparation and purification

ATRA-loaded niosomes are obtained by film hydration method (Santucci et al., 1996).

Briefly, surfactant, Chol and ATRA were mixed in different ratios (Table 1) and dissolved in a chloroform/methanol solution (3:1 v/v). The ATRA loading concentration of 0.5 mg/ml was selected following preliminary studies which highlighted this concentration as the best in terms of ATRA entrapment efficiency into the niosomes (data not shown).

To evaporate the organic phase, a rotary vacuum evaporator (Rotavapor® R-210, Büchi-Italia S.r.l., Assago, MI, Italy) was used up to obtain the 'film'. After, the dried film was hydrated with Hepes buffer (10 mM, pH 7.4) and the obtained dispersion was shaken with a vortex mixer (Vortex-Genie 2, Scientific Industries, Inc., USA) and then sonicated for 5 min, at 60 °C with 20 % of amplitude by using a microprobe operating at 20 kHz (VibraCell-VCX 600-Sonics, Taunton, MA, USA). Finally, the ATRA loaded niosomes were purified by size exclusion chromatography, using Sephadex G75 as column packing material and Hepes buffer as eluent. In particular, the non-encapsulated ATRA and unstructured components were removed by eluting the dispersion of niosomes through the column and the fraction containing the purified sample was collected (dilution 1:5) and analysed (Daneshamouz et al., 2005).

2.3. Physicochemical characterization of ATRA loaded niosomes

After purification, to assure vesicle formation and characterize them in terms of hydrodynamic diameter and ζ-potential, all samples are

Table 1
Sample composition.

Sample	Tw20 (mM)	Tw21 (mM)	Chol (mM)	ATRA (mg/ml)
NT20	15	–	15	0.5
NT20A	15	–	15	0.5
NT21	–	15	15	0.5
NT21A	–	15	15	0.5

analysed using a dynamic light scattering, DLS (Zetasizer Nano ZS 90, Malvern, UK) with a scattering angle of 90.0°and equipped of a 5 mW HeNe laser (λ = 632.8 nm). The vesicle dispersions were diluted 100 times in the Hepes buffer and measured at room temperature.

Concerning the ζ-potential measurements, it was used the Laser Doppler Anemometry, employing the same DLS instrument. The ζ-potential was obtained converting the electrophoretic mobility of the vesicles (u) and using the Smoluchowski relation $\zeta = u\eta/\epsilon$, where η is the viscosity and ϵ the permittivity of the solvent phase (Rinaldi et al., 2015).

ATRA-loaded concentration was measured by UV–visible spectroscopy (Perkin-Elmer, lambda 3a) equipped with a 1.0 cm path-length quartz cell. To begin, different ATRA concentrations were used to establish the calibration curve by using as solvent a hydroalcoholic mixture (Hepes buffer:Ethanol, 30:70, v/v). Then the amount of ATRA was quantified by dissolving loaded samples in the hydroalcoholic solution, by following the absorbance at 344 nm. The entrapment efficiency was determined by the ratio between the amount of ATRA entrapped in the Nio and the amount of ATRA added to niosomes during the preparation procedure.

2.4. Stability studies

Stability over time of all samples was recorded at room temperature and 4 °C for 30 days. Each sample was analysed each day for the first week and then weekly by measuring hydrodynamic diameter and ζ-potential. Moreover, to assure not only the structural stability over time, but also ATRA stability when it is loaded in niosomes, samples were analysed by using the UV–visible spectroscopy and the most significant results were reported (1, 14, 20 and 30 days) (Haddadian et al., 2022; Nerli et al., 2023). Sample stability in presence of cell culture media was evaluated to establish their stability during biological *in vitro* studies. Samples were added to a mix of two different cell culture media, RPMI Dulbecco's Modified Eagles Medium (DMEM) and placed at 37 °C. Samples were analysed at different time intervals (up to 48 h), in terms of particle size and ζ-potential.

2.5. pH-sensitivity: in vitro evaluation using different fluorescent probes

Fluorescence analyses were performed using a Perkin-Elmer LS50B spectrofluorometer on all samples prepared with different fluorescent probes (pyrene, HTPS and calcein), to investigate the vesicle integrity at different pH.

To simulate the physiological condition, Hepes buffer at pH 7.4 was employed, while to mimic the endosomal environment, Acetate buffer at pH 5.5 was used.

1. Pyrene: this hydrophobic probe was used to investigate the micropolarity/microviscosity of vesicular suspension. The probe (4 mM) was added into niosomes at the first preparation step, when the hydrophobic compounds are mixed with the organic solvent. Fluorescence emission spectra were collected from 350 to 550 nm at a λ excitation of 330 nm. The micropolarity was calculated by the ratio of the first (I_1) and the third (I_3) vibrational peaks of the emission spectra which were responsive to the polarity of the surrounding medium (Vasilescu et al., 2011). Instead, the microviscosity was acquired by the ratio between the excimer emission intensity (I_E) and the third vibration band (I_3).
2. 8-Hydroxypyrene-1,3,6-trisulfonic acid trisodium salt: this hydrophilic probe was loaded into the niosomal aqueous core, during the hydration step (0.4 mM in Hepes buffer). According to the literature (Kano and Fendler, 1978), the fluorescence intensity of HPTS is strongly dependent upon the degree of ionization of the 8-hydroxyl group (pKa = 7.2) and consequently to the pH environment. For HPTS experiments, the excitation spectra (350–500 nm) was

followed at an emission wavelength of 510 nm and the emission spectra (450–600 nm) was taken at an excitation wavelength of 400 nm.

3. Calcein release assay: in this experiment, the calcein leakage percentage was assessed to evaluate the pH sensitivity and the stability of ATRA-loaded Nio in human serum at different pH. Firstly, the samples have been prepared as described in section 2.2 and hydrated with calcein solution (10 mM in Hepes buffer, pH 7.4). The dye encapsulated in the niosomal core is at self-quenched concentration. An aliquot of sample was added to buffer solutions (1:10, v/v) at different pH values (7.4 and 5.5), in absence (0 %) or in presence of 50 % of human serum (Kobanenko et al., 2022). This mixture was incubated at 37° C under constant stirring, for 3 h. Calcein leakage was evaluated after 3 h. The calcein fluorescence analysis was measured at λex = 490 and λem = 520 nm, before and after the addition of isopropanol (1:1, v/v). Fluorescence intensities measured at acidic pH values were corrected for the slight effect of pH on calcein fluorescence. The calcein leakage percentage (CL%) was calculated using the following equation:

$$CL\% = \frac{I\,pH - I0}{I\,100 - I0} \times 100 \qquad (1)$$

where I_{pH} is the intensity measured at acidic pH before the addition of isopropanol, I_{100} is the totally dequenched calcein fluorescence at neutral pH and I_0 is the fluorescence at neutral pH (Simoes et al., 2001).

2.6. Structural characterization

The structural properties of Nio on the nanoscale have been investigated by Small Angle X-Ray Scattering (SAXS) technique. Measurements were performed at the BM26 beamline (ESRF, Fr), experiment MD-1386. Samples were put in plastic capillaries (ENKI, Concesio, Italy) and the scattered radiation was acquired at two different sample-to-detector distances (1.4 and 9 m) to measure the scattered intensity spectra I(q) in a wide q region (0.022–7.5 nm^{-1}). The momentum transfer q is q = $2\pi/\lambda$ sin($\theta/2$), λ being the wavelength of the incident radiation and θ the scattering angle. The measure of I(q) in this wide q-range can reveal the structure of the Nio from the overall shape (hundreds of nms) to the internal details (nms). The internal organization has been modeled by a bilayer form factor (heads-chains-chains-heads) suitable to fit the intensity profile in the high-q region (Doucet et al., 2019).

2.7. Morphological analysis

To directly visualize synthesized niosomes, their shape and morphological features, niosomal dispersions were investigated by negative staining under a transmission electron microscope. A drop of each niosomal sample was applied on a 400-mesh formvar-coated copper grid and allowed to adhere for 1 min. After blotting the grid with a filter paper, a drop of 2 % (v/v) filtered aqueous sodium phosphotungstate acid (PTA) (pH 7.4) was applied for 1 min. The remaining solution was then removed, the samples air dried and examined by a FEI 208S TEM (FEI Company, Hillsboro, OR, USA), equipped with the Megaview II SIS camera (Olympus, Hamburg, Germany), at an accelerating voltage of 100 kV. Adobe Photoshop software (Adobe, San Jose, CA, USA) was used to optimize image editing.

2.8. ATRA release studies

In vitro release of ATRA from niosomal formulations was investigated using cellulose dialysis tubing (MWCO 8 kDa, Spectra/Por®, Rancho Dominguez, CA, USA). The sample and 45 % of Hepes buffer or Acetate buffer were placed in a dialysis bag and then immersed into the release medium (Hepes buffer: Ethanol, 30:70, v/v). The release system was

constantly stirred with a magnetic bar (100 rpm) at 37 °C. At pre-determined intervals (from 0 to 8, each hour and 24 h), an aliquot of release media was withdrawn, measured, and replaced into the release medium. The released ATRA from niosomes was analysed by UV–visible spectrophotometer as described before.

2.9. Cell lines and treatments

OVCAR-3 were purchased from ATCC whereas OVSAHO from JCRB. Kuramochi were kindly provided by Professor S. Indraccolo. OVCAR-3 were maintained in DMEM (#SD6546-500 mL – Sigma-Aldrich, St. Louis, MO, USA) supplemented with 20 % Fetal Bovine Serum (Gibco, Carlsbad, CA, USA), 1 % Glutamine (#G7513-100 mL – Sigma-Aldrich), 10 mM Hepes (#H0887-100 mL – Sigma-Aldrich), 1 mM sodium pyruvate (#S8636-100 mL – Sigma-Aldrich) and 0.001 mg/mL Insulin (#I9278-5 mL - Sigma-Aldrich). Kuramochi and OVSAHO were maintained in RPMI-1640 (#R0883-500 mL – Sigma-Aldrich, St. Louis, MO, USA) supplemented with 10 % Fetal Bovine Serum (Gibco), and 1 % Glutamine (#G7513-100 mL – Sigma-Aldrich). All cell lines are mycoplasma-free.

Cells were treated with different doses (as indicated in some Figures) of all-trans retinoic acid [ATRA (#R2625 – Sigma-Aldrich) for 96 h (48 h + 48 h: after 48 h medium was replaced and cells were treated for additional 48 h), according to its datasheets' instructions.

2.10. Cell viability

To analyse the cytotoxicity of blank niosomes, OVCAR3, Kuramochi, and OVSAHO were plated in 96-well plates at 5x10^4, 3x10^4, 7x10^4 density, respectively. Cells were treated the day after with increasing doses of the indicated blank niosomes for 96 h (48 h + 48 h). At the end of the treatment, cell viability was determined using CellTilter 96(R) AQueous One Solution Assay (PRO-G3580 – Promega, Fitchburg, WI, USA) by Glomax Discover Microplate Reader (Promega).

To evaluate whether ATRA-loaded niosomes affect cell growth, cells were harvested at the end of the treatment and counted by using a Trypan blue assay.

2.11. Western blot analysis

Total protein extract preparation (Giuli et al., 2020a) and immuno-blot assay with the specific antibodies (Pelullo et al., 2019) were performed as described elsewhere. For total protein extracts, cells were lysed in Lysis buffer (50 mM Tris HCl (pH 7.5), 150 mM NaCl, 1 mM EDTA, 0.5 % Triton X-100, 10 mM NaF, 1 mM Na_3VO_4, 1 mM PMFS, 1 % Protease inhibitors) and clarified at 13.000 × rpm for 15 min. Before immunoblotting samples were added with β-mercaptoEthanol (#M6250 – Sigma-Aldrich) and boiled for 5 min. For immunoblotting, protein extracts were run on SDS-polyacrylamide gels and transferred to nitro-cellulose membranes (#1620115 – Biorad, Hercules, CA, USA). Blots were then incubated with several primary antibodies. From Santa Cruz Biotechnology (Dallas, TX, USA): anti-Pin1 (#sc-46660) and anti-vinculin (#sc-25336); from Sigma-Aldrich: anti-β-actin (#A5316). The blots were then incubated with secondary antibodies HRP-conjugated: anti-rabbit (#JI111035003 – Jackson ImmunoResearch, West Grove, PA, USA) or anti-mouse (#7076S – Cell Signalling Technology, Beverly, MA, USA). Bound antibodies were detected with enhanced chemiluminescence (#170-5061 – Biorad, Hercules, CA, USA).

2.12. Statistical analysis

Results are expressed as mean ± SD. All statistical tests were carried out by using GraphPad Prism version 7.0 (GraphPad Software, San Diego, California, USA).

Multiple comparison analyses were determined using unpaired Student's *t* test or ordinary one-way ANOVA followed by Tukey's or Dunnett's post-hoc tests and statistical significance was set at P ≤ 0.05. Results are expressed as mean ± SD from an appropriate number of experiments (at least three biological replicates). Values significance: ns = not significant P > 0.05, *P ≤ 0.05, **P ≤ 0.001, ***P ≤ 0.0001.

3. Results and discussion

Since the discovery of Vitamin A in 1913 by McCollum and Davis to now, several researchers have shown the key role of ATRA in numerous physiological processes in vertebrates as well as its chemotherapeutic and chemopreventive effects in several types of tumor. Despite the promising effects, the use of this molecule for therapeutic purposes is still difficult due to its chemical limitations, such as low aqueous solubility (0.21 μM at pH 7.3 (Szuts and Harosi, 1991), photodegradation or instability in the human serum, as well as its toxicity.

In ovarian cancer field, the search for an alternative way to handle ATRA acquires great interest to open novel strategies for the treatment, currently still not totally effective.

To this aim, two different surfactant-based nanocarriers composed by Tween 20 (Tw20) or Tween 21 (Tw21) have been formulated and deeply characterised. These niosomes have been chosen because our previous studies have highlighted their high stability over time and in the biological fluids (Di Marzio et al., 2011), their ability to efficiently entrap lipophilic/hydrophilic drugs (Hanieh et al., 2022; Rinaldi et al., 2019) and the pH-sensitiveness of Tween 21 (Di Marzio et al., 2011).

In the present work, these formulations have been loaded with ATRA (ATRA-loaded niosomes, NT20A or NT21A) and characterised in terms of vesicle formation, pH-sensitivity, serum stability and drug release at different pH values, in Hepes buffer (to mimic the bloodstream, pH 7.4) *versus* Acetate buffer (to mimic the endosomal environment, pH 5.5).

A deep physico-chemical characterization of drug-loaded niosomes represents a fundamental step to establish the feasibility of these structures for therapeutic purposes, to explain their behaviour *in vitro* and to predict their effective application for future *in vivo* studies.

3.1. Vesicle formation and characteristics

The surfactant vesicles, prepared with a mixture of amphiphilic substances (Tw 20 or Tw 21), Chol, at same molar ratio, and ATRA were obtained by the film method, purified by using size exclusion chromatography and characterised.

Generally, the hydrophilic surfactants, with hydrophilic-lipophilic balance (HLB) value higher then 14, are not suitable to form a bilayer membrane because of their aqueous solubility. However, from our previous studies, niosomes constituted by Tw20/Tw21 (NT20/NT21) are able to form stable vesicles if in equimolar presence of cholesterol concentration (Di Marzio et al., 2011). This data was also confirmed in the present study by the DLS analysis (Table 2) and SAXS investigation (Fig. 1).

DLS results show that both surfactants, in the presence of cholesterol, were able to form nano-sized structures with different hydrodynamic diameters: 251 nm for NT20A and 190 nm for the NT21A (Table 2). Moreover, all vesicles showed a size distribution nearly monodisperse (PDI ≤ 0.4) (Rahat et al., 2021).

Table 2

Vesicle dimensions (hydrodynamic diameter), polydispersity index (PDI), Z-potential values, ATRA entrapment efficiency percentage related to the loaded amount (% EE). Reported data are means of three.

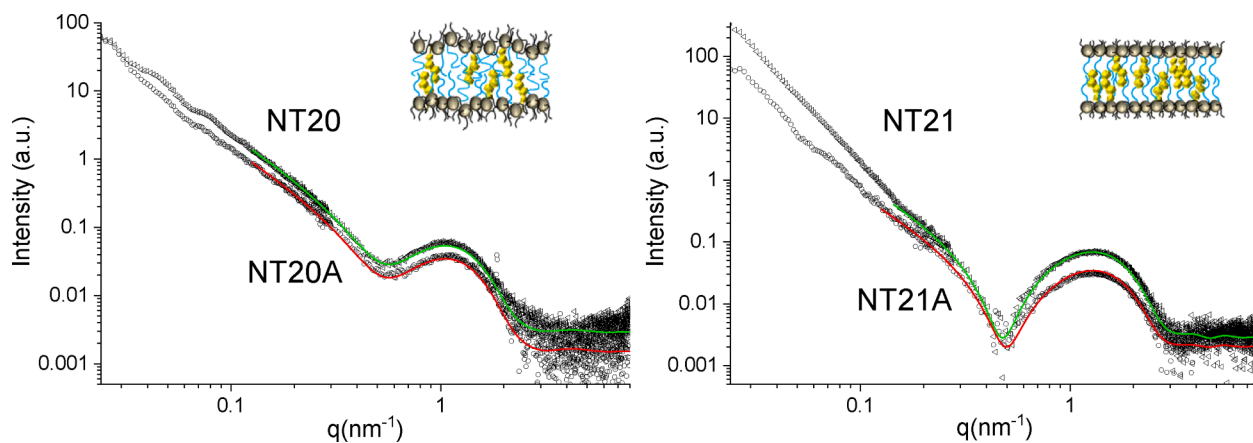| Sample	Hydrodynamic diameter (nm) ± SD	Z-Potential (mV) ± SD	PDI ± SD	ATRA EE (%)	ATRA loaded (mg/ml)
NT20	281 ± 2	−40 ± 2	0.3	–	–
NT20A	251 ± 2	−30 ± 2	0.4	16	0.08
NT21	175 ± 3	−43 ± 2	0.3	–	–
NT21A	190 ± 1	−40 ± 1	0.4	12	0.06

Fig. 1. SAXS spectra of niosomes at 25 °C. Lines represent the fit of the bilayer form factor in the 0.12–8 nm^{-1}q region for unloaded (green) and ATRA-loaded (red) systems. On the left are reported SAXS spectra for Tween 20 niosomes and on the right are reported the ones for Tween 21 niosomes. (For interpretation of the references to colour in this figure legend, the reader is referred to the web version of this article.)

According to the literature, the vesicular diameter depends on two parameters: the alkyl chain length and HLB value of non-ionic surfactant (Tw20 HLB: 16.7; Tw21 HLB: 13.3). Typically, non-ionic surfactants with higher HLB are able to form large vesicles (Yoshioka et al., 1994), therefore the smaller size of NT21A compared to the NT20A one might be related to the lower HLB of Tw21, which confers to the system a higher hydrophobicity, thus causing a decrease of the surface-free energy (Di Marzio et al., 2011). SAXS spectra of NT20 and NT21 are reported in the Fig. 1: the intensity profiles show the typical features of

vesicular particles, with overall size in agreement with DLS results.

The internal structure of Nio has been modelled with a bilayer form factor, heads-chains-chains-heads. The best fits are reported in the Fig. 1. The bilayer of NT20 niosomes is about 6 nm thick (2–1-1–2 nm), with a rough surface (0.3 polydispersity) due to the presence of the branched and highly hydrated heads of Tw20. NT21 shows a more defined, thinner bilayer (thickness 5.2 nm) as expected for shorter polyoxyethylene hydrophilic chains (Table S1).

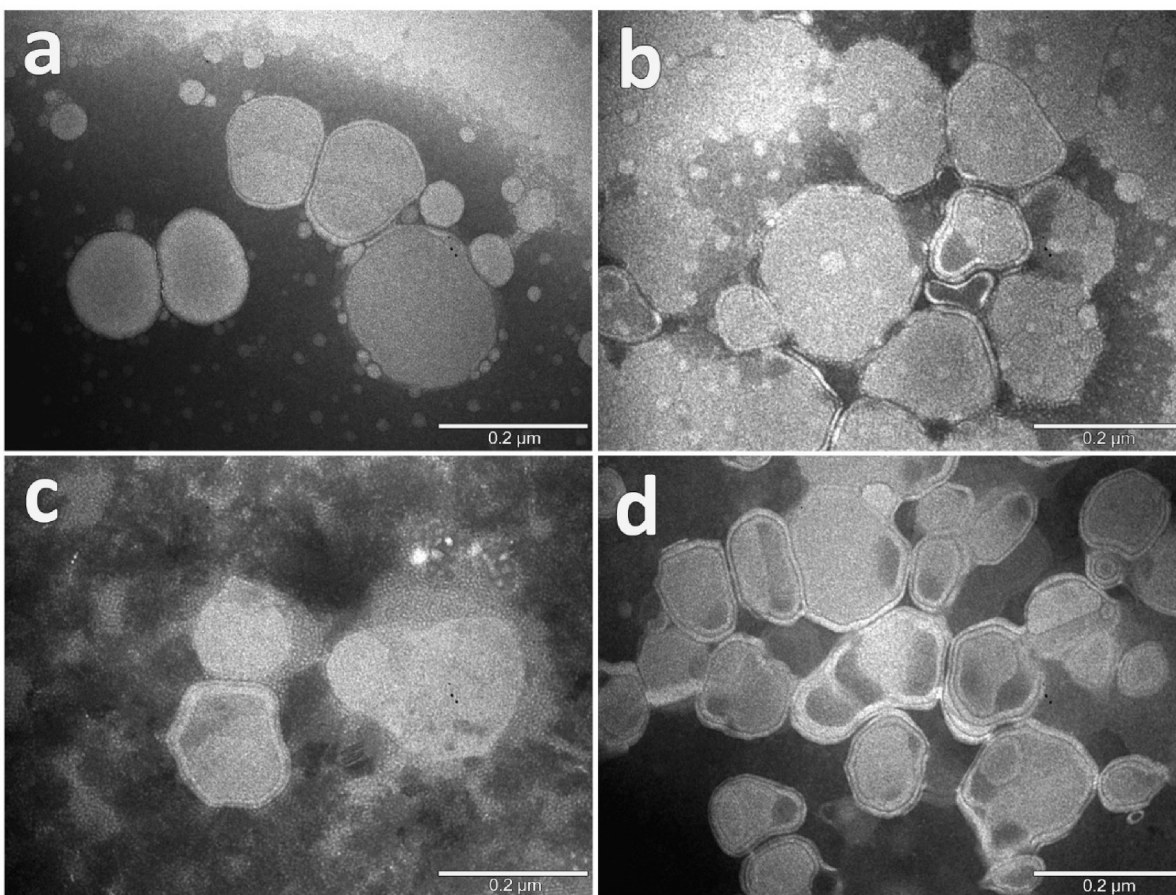ATRA loading doesn't affect dramatically the size and shape of

Fig. 2. Transmission electron micrographs of empty and ATRA-filled niosomal samples. Vesicles were counterstained with PTA and observed as negative staining. Panels a and b: NT20 and NT20A, respectively; panels c and d: NT21 and NT21 A, respectively.

niosomes. A small decrease in size is observed for NT20A (251 nm) and a small increase in size for NT21A (190 nm).

Also, the internal structure of the niosomes keeps the main features, thickness of both NT20A and NT21A bilayers staying the same. The effective entrapment of ATRA is proved by a slight change of the electron density of the bilayers.

The presence of ATRA within the hydrophobic chains of the bilayers may affects the packing of the components, for instance causing a different transverse distribution of cholesterol within the two layers, which could induce a different curvature of the bilayer and thus a size change of the niosomes.

All formulations have similar negative ζ-potential values (Table 2), ranging from −30 to −40 mV, preventing vesicle aggregation during the storage due to the superficial electrostatic repulsion (Müller et al., 2001). According to the literature (Moraru et al., 2020), a ζ-potential value larger than ± 20 mV assures sample stability.

Both vesicular nanocarriers are able to incorporate ATRA with a comparable entrapment efficiency (Table 2): 16 % of loading concentration, corresponding to ATRA concentration of 0.08 mg/ml for NT20A and 12 % of loading concentration, corresponding to ATRA concentration of 0.06 mg/ml for and NT21A. In the selected formulations the entrapped ATRA concentration is higher than the concentration of free ATRA necessary to observe a cellular effect on Pin 1, as shown by Russo Spena and colleagues (10 μM, ≈ 0.003 mg/ml) (Spena et al., 2018).

To directly visualize niosome vesicles and confirm the particle assembly revealed by SAXS investigation, a morphological analysis by TEM was performed (Fig. 2). Blank samples (Panels a and c) showed that both Tw20 and 21, together with cholesterol, assembled into vesicular nanostructures with almost spherical shape and size compatible with DLS measurements, also taking into account the dehydration due to the electron microscope procedure. NT20 and NT21 filled with ATRA (Panels b and d) were shown to maintain the original spherical shape and morphology, with some vesicles appearing partially deformed, perhaps due to the more flexible surface structure, as highlighted by SAXS analysis.

3.2. Stability studies

One of the main issues in the design of nanocarriers to deliver the high lipophilic ATRA molecule is its instability in the aqueous environment. Moreover, ATRA is well known to be a molecule very sensitive to heat, light, and oxidation (Trapasso et al., 2009). Indeed, even after an "apparently" efficient loading, the poorly-soluble ATRA molecules often tend to deposit on or near the surface of nanocarriers, leading to significant burst releases of ATRA in the aqueous environment leading to a fast degradation (Narvekar et al., 2012). For this reason, the evaluation

of protective effect over time of niosomal bilayer towards the entrapped ATRA molecule was a crucial point.

The stability of ATRA loaded into niosomes was investigated over 30 days, by assessing both vesicle stability, in terms of hydrodynamic diameter and ζ-potential (Fig. 3, panel A), and simultaneously checking ATRA concentration by UV–vis spectra (Fig. 3, panel B).

As shown in Fig. 3A, all formulations displayed no relevant variations of both checked parameters during the storage period at both temperatures. Similar data were obtained for unloaded niosomes (Figure S1, Supporting Information).

When the formulations were stored at room temperature, we observed that ATRA concentration decreased: in particular, for NT20A starting from the day 14, the concentration moves from 0.08 to 0.05 mg/ml, until to 0.038 mg/ml after 30 days (Fig. 3B), therefore the ATRA stability was less than 14 days. While, for the NT21A, this phenomenon was evident only after 30 days when ATRA concentration slightly decreased from 0.06 to 0.043 mg/ml. On the other hand, formulations stored at 4 °C were stable. These data showed that ATRA remained durably entrapped after 30 days of storage indicating no significant drug leakage from niosomes. Cuomo and co-workers (Cuomo et al., 2021) observed that after 3 days of storage the absorbance spectra of free ATRA, both refrigerated or stored at room temperature, were lower than for the starting solution. Therefore, the concentration decreased with storage time, but the temperature did not affect ATRA degradation.

Taking into consideration these results, the niosomal bilayer confers suitable protection to ATRA molecule, without adding to the formulation the antioxidants such as α-tocopherol (Brisaert et al., 2001).

3.3. pH sensitivity evaluation

The physical state of the bilayer plays a critical role in the retention of niosomal content as well as in their circulation time *in vivo* (Senior and Gregoriadis, 1982). The sensitivity to acidic pH of empty niosomes composed by Tw20 or Tw21 has been already evaluated and Tw21 niosomes showed pH-sensitiveness (Di Marzio et al., 2011).

The pH-sensitivity of niosomes was investigated employing three different fluorescent probes: Pyrene, HTPS and Calcein.

Due to the hydrophobic nature of Pyrene, it was co-localized with ATRA into the niosomal bilayer. Pyrene spectra allow to collect information on bilayer micropolarity and microviscosity.

From data obtained by analysing the Pyrene spectra of niosomes in the presence of ATRA (Table 3), we observed an increase of micropolarity (ratio I_1/I_3) at acidic pH when compared to the physiological one. Generally, an increase of this ratio indicated an increase of self-assembling organisation. At acidic pH, a bilayer destabilisation should occur with a formation of mixed aggregates that could generate
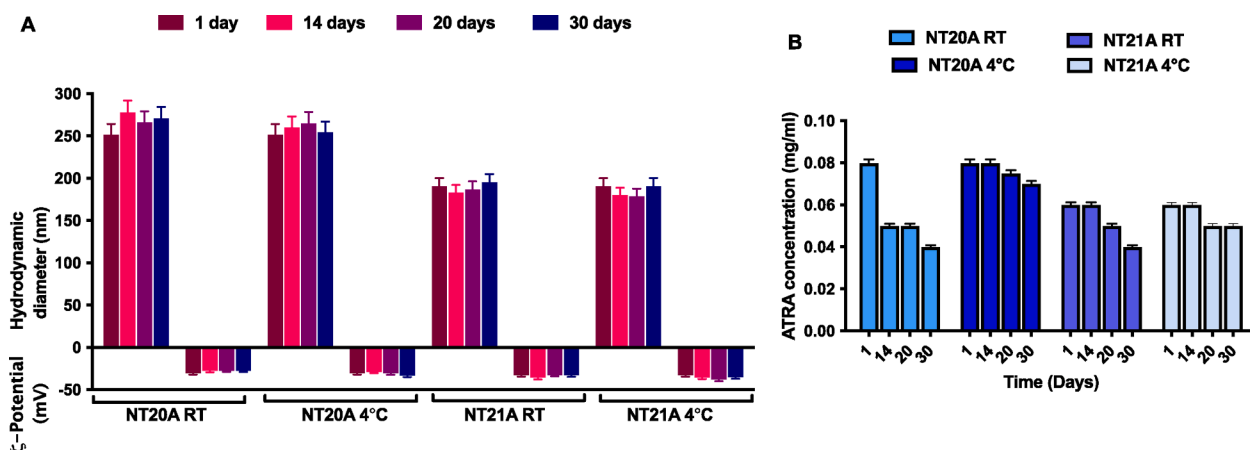

Fig. 3. Effects of storage on ATRA encapsulation into niosomes. The samples are analysed by using DLS and UV–vis spectrophotometer. RT - Room Temperature. Reported data represent the mean of three experiments. (A) Stability of vesicular structure over time; (B) ATRA stability over time.

Table 3
Bilayer features of all samples after pyrene addition at different pH media. Reported data represent the mean of three experiments.

Sample	Buffer	Micropolarity (I_1/I_3)	Microviscosity (I_E/I_3)	Hydrodynamic diameter (nm)
NT20A	Hepes	1.60	0.15	251
	Acetate	1.70	0.07	810
NT21A	Hepes	1.59	0.19	190
	Acetate	1.65	0.07	672

hydrophobic regions providing clusters in which the probe might be trapped (Jones et al., 2003). Accordingly, this may induce an increase of the hydrodynamic diameter as confirmed by DLS measurements (Table 3) (Na et al., 2004).

The microviscosity is a parameter inversely proportional to bilayer fluidity (Turro and Kuo, 1986). As shown in the Table 3, the ratio I_E/I_3 decreased at acidic pH, highlighting an increase of membrane fluidity. According to Shinitzky and co-workers (Shinitzky and Barenholz, 1978), a high membrane fluidity is correlated to a low structural order, so it is possible to conclude that in the presence of ATRA and acidic pH, both bilayer structures seemed to be destabilised. Empty niosomes have been analysed and obtained data confirmed our previous results: NT21 are pH-sensitive systems, which become unstable in response to changes of pH environments (Di Marzio et al., 2011).

To confirm these results, the hydrophilic probe HTPS was added to the niosomal aqueous core after ATRA inclusion, and its excitation and emission spectra were recorded at both pHs.

As shown in the Fig. 4, at 450 nm the peak of pyranine disappeared when the samples NT20A and NT21A were in the presence of acidic pH. According to Kano and Fendler (Kano and Fendler, 1978), these data suggested a destabilization of vesicular structure, with the escape of HTPS, previously localized in the inner niosomal aqueous core, in the acidic external medium.

Together with the pH-sensitivity evaluation, the serum stability represents an important parameter to assess the potential *in vivo* use of a nanocarrier, thus improving the drug delivery into cellular cytoplasm (Fattal et al., 2004).

The major concern about pH-sensitive formulations is their relative instability in plasma or serum (Roux et al., 2002), with premature drug leakage (Liu and Huang, 1989).

Niosome stability was evaluated by monitoring the calcein release. The fluorescent probe is encapsulated in niosomes at self-quenched concentration and its leakage, due to vesicle perturbation, can cause its dilution in the buffer, giving an increase of fluorescence (Simoes et al., 2001). Furthermore, to better mimic the *in vivo* environments, all samples were analysed at different pH and in the presence of 0 % and 50 % of human serum. As shown in the Fig. 5, the addition of serum to all formulations did not significantly alter the calcein leakage, thus confirming the stability of all vesicles at pH 7.4 and indicating that the nanocarrier should be stable enough to reside in the blood stream for a prolonged time.

Formulations showed a strong increase of calcein leakage at acidic pH, except for the sample NT20, confirming previously reported data on similar systems (Di Marzio et al., 2008).

Experimental results suggest that the pH-sensitivity of ATRA-loaded niosomes could be related to a bilayer perturbation. This phenomenon was maintained in the presence of serum and the increase of calcein leakage is probably related to the increase of bilayer fluidity (Carafa et al., 2006). Moreover, the presence of ATRA, localized into the niosomal bilayer, may contribute to the formation of less resistant structures (Manconi et al., 2002).

These findings suggest a probable niosomal efficacy in ATRA cytoplasmic delivery, and their stability in human serum.

3.4. In vitro ATRA release studies

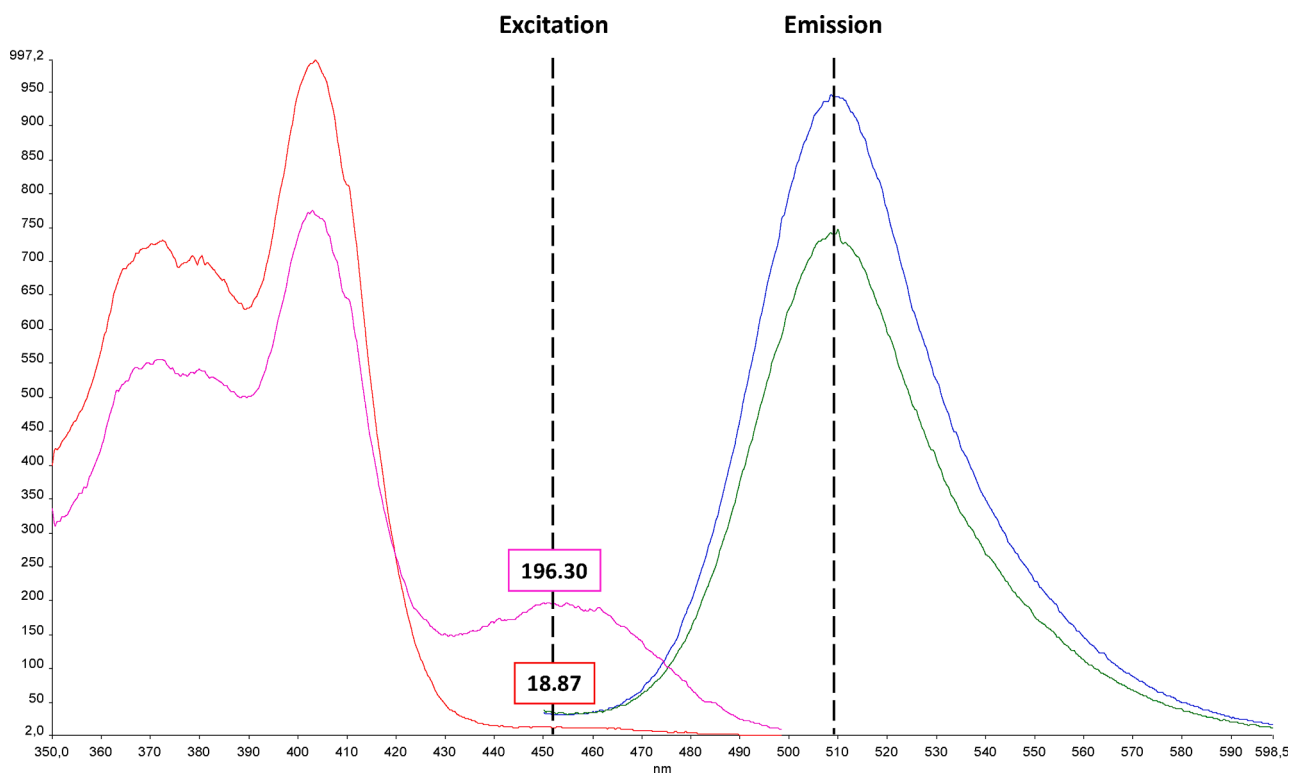The *in vitro* drug release profile of ATRA was determined by the

Fig. 4. HPTS spectra of sample NT21A. Excitation (450 nm) and emission spectra (520 nm) at pH 7.5 (pink/blue lines) and at pH 5.5 (red/green lines). The HTPS spectra obtained with NT20A, shown the similar trend. Reported data represent the mean of three experiments. (For interpretation of the references to colour in this figure legend, the reader is referred to the web version of this article.)
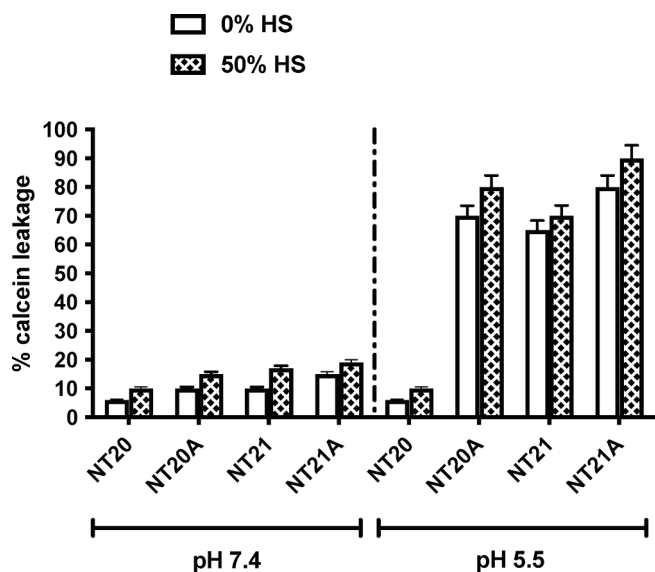
Fig. 5. Calcein release assay. Influence of the absence (0 %) and presence (50 %) of Human Serum (HS) on the stability and pH-sensitivity of all samples at 37 °C, in two different pH media. Reported data represent the mean of three experiments.

membrane diffusion method in the presence of both selected media (Fig. 6). After 24 h, at pH 7.4, a gradual drug release was observed for both formulations. On the other hand, when the formulations were placed at pH 5.5, a burst ATRA release was observed up to the total release, after 24 h and 4 h for NT20A and NT21A, respectively (Grace et al., 2021).

This result could be due to a higher bilayer permeability of niosomes at acidic pH, in accordance with the microviscosity values (Table 3) (Yoshioka et al., 1994).

3.5. Enhanced ATRA efficacy after niosomes encapsulation

We next compared ATRA-loaded niosomes with free ATRA *in vitro*. While the anti-oncogenic effects of ATRA have been previously evaluated in HGSOC cell lines including Kuramochi (Coscia et al., 2016)

and (Lokman et al., 2019; Losi et al., 2019) OVCAR-3 cells, to the best of our knowledge, this is the first investigation of ATRA inhibitory activity of Pin1 in HGSOC context. Indeed, ATRA-dependent Pin1 inhibition was evaluated only on OVCAR-3 by Russo Spena and colleagues, but they did not obtain striking results with respect to other Pin1 inhibitors (Russo Spena et al., 2019; Spena et al., 2018).

Therefore, we first assessed the free ATRA effects on Pin1 protein expression levels on three HGSOC cell lines (Kuramochi, OVCAR-3 and OVSAHO) which resemble with varying degrees the tumor profile of HGSOCs (Domcke et al., 2013). Notably, ATRA treatment did not exert Pin1 inhibition in OVSAHO (Fig. 7A) and Kuramochi (Fig. 8A) cell lines within the tested concentration (0.0015 mg/ml – 0.0030 mg/ml – 0.0060 mg/ml) whereas we observed a modest decrease in the level of the Pin1 protein in OVCAR-3 cells at high concentrations (0.0030 mg/ml – 0.0060 mg/ml) (Fig. 9A), thereby supporting the need of improving ATRA delivery to achieve an efficient Pin1 inhibition. To determine whether the ATRA-loaded niosomes are more effective than free ATRA in HGSOC cells, we first assessed the effects of the blank niosomes on the viability of HGSOC cells, after evaluating the noisome integrity in culture media (Figure S2). Notably, NT20 showed no significant cell toxicity on Kuramochi and OVCAR-3 (Figs. 8 and 9, panels B) and only modest cell toxicity (>70 % viability) at the highest concentration, corresponding to NT20 containing ATRA 0.0060 mg/ml on OVSAHO cells (Fig. 7B). With respect to the treatment with NT21, it resulted in higher toxicity across all cell lines with no effect at the lowest concentration (Figs. 7-9, panels C). This was probably due to the lower ATRA entrapment efficiency (Table 2) which resulted in higher amounts of structured Tween 21 with respect to structured Tween 20 corresponding to the same ATRA payload. Collectively, we chose the lowest concentration for both blank niosomes, thus excluding that the hypothesised enhanced effects, potentially observable after treatment with ATRA-loaded niosomes, could be caused by inherent carrier toxicity. We next evaluated the effects of the blank niosomes on Pin1 protein expression in the same experimental conditions. As shown in the panel D of both Figs. 8 and 9, blank niosomes did not cause a decrease in the level of Pin1, with the only exception of NT21-treated OVSAHO cells (Fig. 7D).

We next compared the effects of ATRA-loaded niosomes with free ATRA. Interestingly, they induced a significant down-regulation of Pin1 protein levels with respect to free ATRA in all the cells analysed (Figs. 7-
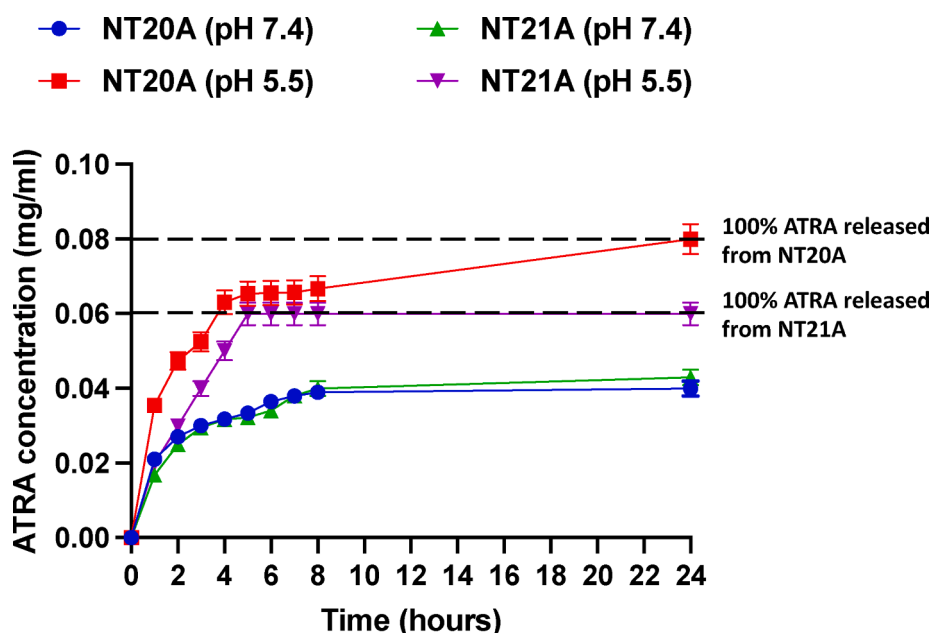

Fig. 6. ATRA release profile from niosomes at different pH media. The data represent the means for three replicate samples of three separate experiments.
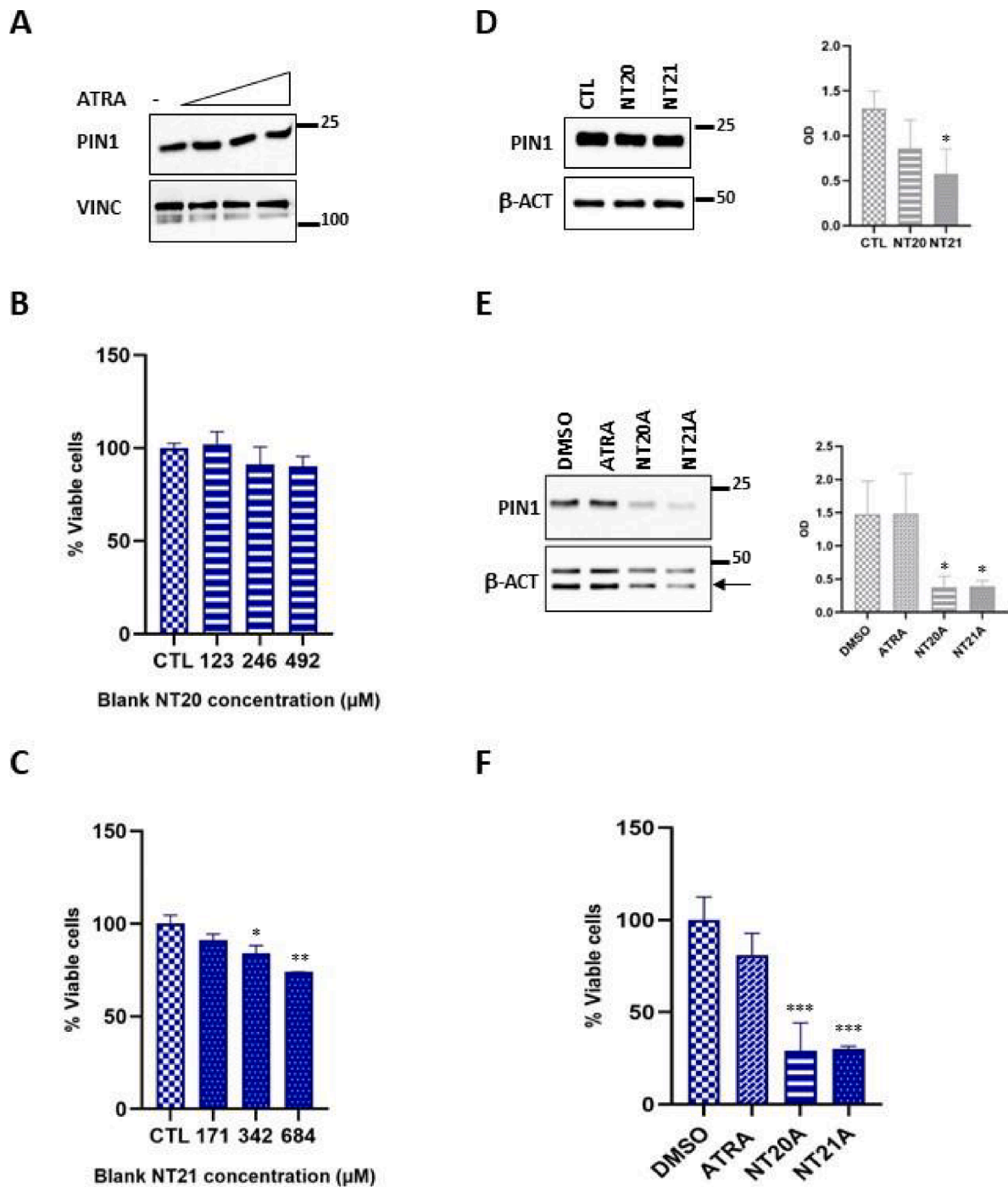
Fig. 7. *In vitro* studies on OVSAHO. **(A)** Western Blot analysis showing Pin1 endogenous protein levels in OVSAHO cells treated with the indicated doses of ATRA for 96 h (48 h + 48 h). **(B – C)** Cell viability assay on OVSAHO cells treated with the indicated concentration of NT20 and NT21 expressed as structured surfactant corresponding to ATRA-loaded niosomes containing 0.0015 mg/ml – 0.0030 mg/ml – 0.0060 mg/ml ATRA, respectively, for 96 h (48 h + 48 h). The results are expressed as the mean average deviation of %viable cells of three separate experiments and P-values were calculated using ordinary one-way ANOVA followed by Dunnett's post-hoc test. **(D)** Left panel - western blot analysis showing Pin1 endogenous protein levels in OVSAHO cells treated with NT20 123 μM and NT21 171 μM for 96 h (48 h + 48 h); **right panel** - graphs showing the relative quantification as determined by optical densitometry (OD). The results are expressed as the mean average deviations of three separate experiments and P-values were calculated using ordinary one-way ANOVA followed by Tukey's post-hoc test. **(E)** Left panel - western blot analysis showing Pin1 endogenous protein levels in OVSAHO cells treated with ATRA 0.0015 mg/ml, NT20A 0.0015 mg/ml, and NT21A 0.0015 mg/ml for 96 h (48 h + 48 h); **right panel** – graphs showing the relative quantification as determined by optical densitometry (OD). The results are expressed as the mean average deviations of three separate experiments and P-values were calculated using ordinary one-way ANOVA followed by Tukey's post-hoc test. **(F)** Cell survival of OVSAHO cells treated with ATRA 0.0015 mg/ml, NT20A 0.0015 mg/ml, and NT21A 0.0015 mg/ml for 96 h (48 h + 48 h). The results are expressed as the mean average deviation of %viable cells of three separate experiments and P-values were calculated using ordinary one-way ANOVA followed by Tukey's post-hoc test. In **(A)**, **(D),** and **(E)** anti-Pin1 antibody was used to detect Pin1 protein levels, and anti-ß-actin or anti-vinculin antibodies were used as a loading control. In **(B - E)** values significance: ns = not significant $P > 0.05$, *$P \leq 0.05$, **$P \leq 0.001$, ***$P \leq 0.0001$.
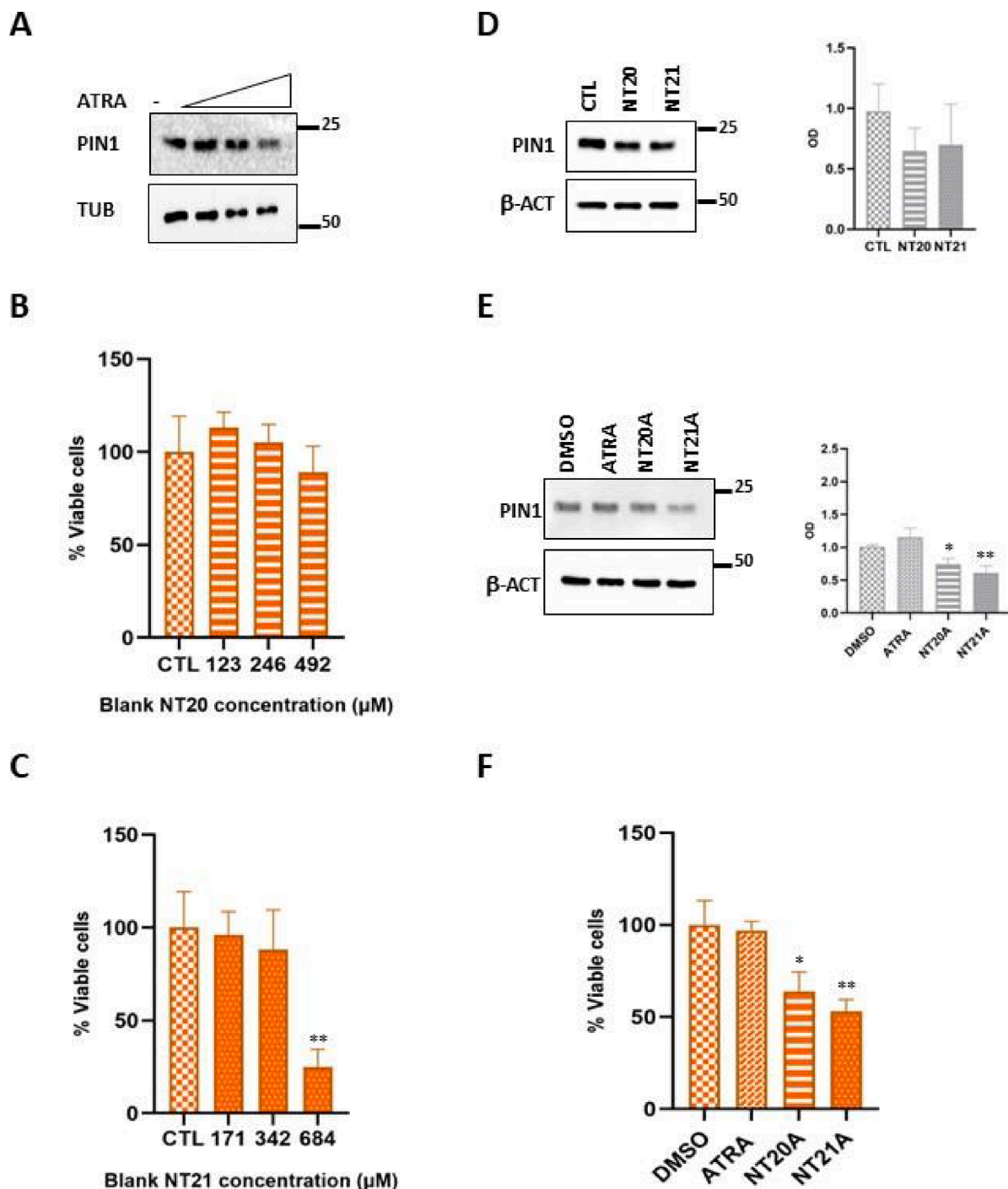
Fig. 8. *In vitro* **studies on Kuramochi.** **(A)** Western Blot analysis showing Pin1 endogenous protein levels in Kuramochi cells treated with the indicated doses of ATRA for 96 h (48 h + 48 h). **(B – C)** Cell viability assay on Kuramochi cells treated with the indicated concentration of NT20 and NT21 expressed as structured surfactant corresponding to ATRA-loaded niosomes containing 0.0015 mg/ml – 0.0030 mg/ml – 0.0060 mg/ml ATRA, respectively, for 96 h (48 h + 48 h). The results are expressed as the mean average deviation of %viable cells of three separate experiments and P-values were calculated using ordinary one-way ANOVA followed by Dunnett's post-hoc test. **(D) Left panel** - western blot analysis showing Pin1 endogenous protein levels in Kuramochi cells treated with NT20 123 μM and NT21 171 μM for 96 h (48 h + 48 h); **right panel** - graphs showing the relative quantification as determined by optical densitometry (OD). The results are expressed as the mean average deviations of three separate experiments and P-values were calculated using ordinary one-way ANOVA followed by Tukey's post-hoc test. **(E) Left panel** - western blot analysis showing Pin1 endogenous protein levels in Kuramochi cells treated with ATRA 0.0015 mg/ml, NT20A 0.0015 mg/ml, and NT21A 0.0015 mg/ml for 96 h (48 h + 48 h); **right panel** - graphs showing the relative quantification as determined by optical densitometry (OD). The results are expressed as the mean average deviations of three separate experiments and P-values were calculated using ordinary one-way ANOVA followed by Tukey's post-hoc test. **(F)** Cell survival of Kuramochi cells treated with ATRA 0.0015 mg/ml, NT20A 0.0015 mg/ml, and NT21A 0.0015 mg/ml for 96 h (48 h + 48 h). The results are expressed as the mean average deviation of %viable cells of three separate experiments and P-values were calculated using ordinary one-way ANOVA followed by Tukey's post-hoc test. In **(A)**, **(D)**, and **(E)** anti-Pin1 antibody was used to detect Pin1 protein levels, and anti-ß-actin or anti-tubulin antibodies were used as a loading control. In **(B - E)** values significance: ns = not significant $P > 0.05$, *$P \leq 0.05$, **$P \leq 0.001$, ***$P \leq 0.0001$.
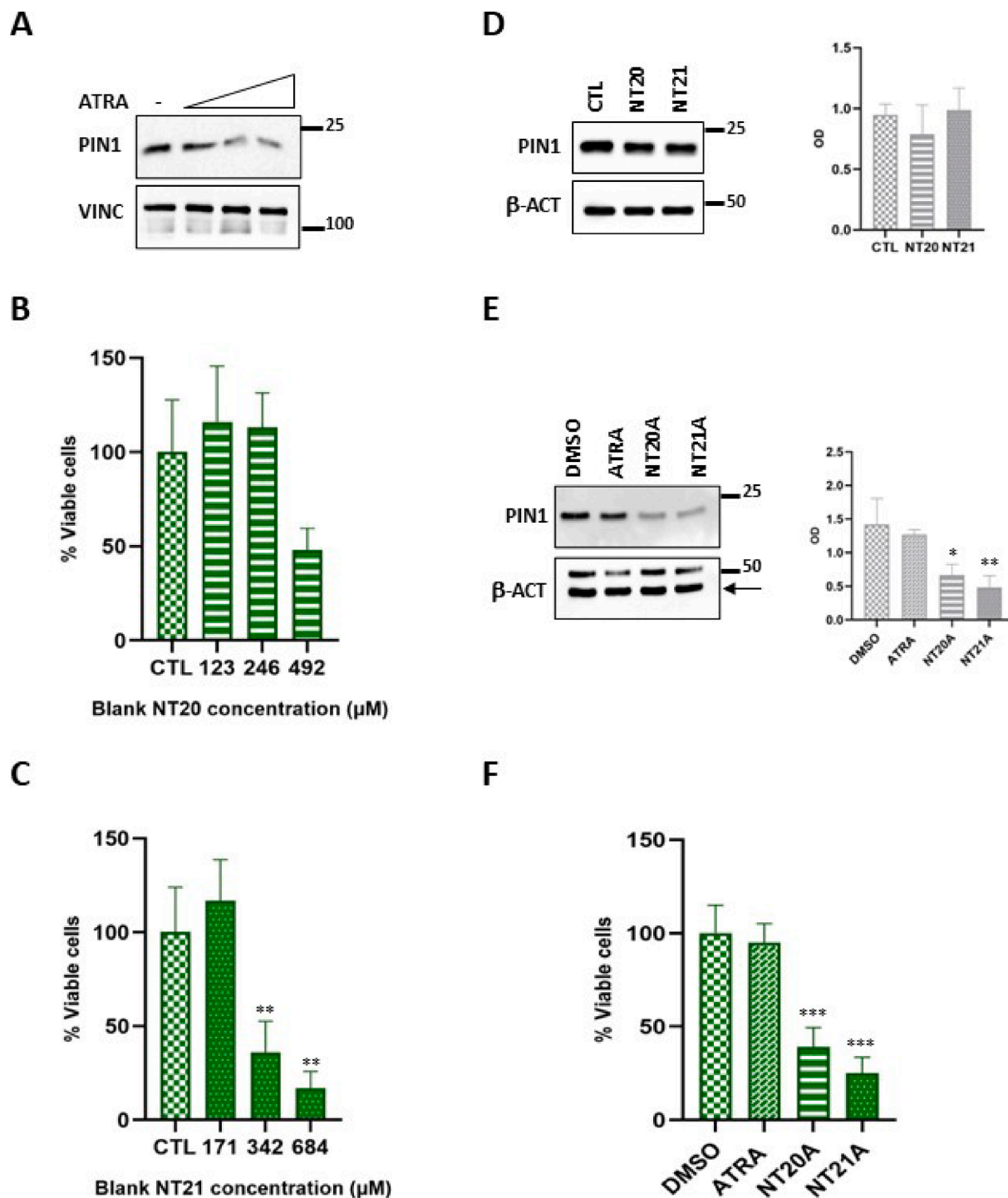
Fig. 9. *In vitro* studies on OVCAR-3. (A) Western Blot analysis showing Pin1 endogenous protein levels in OVCAR-3 cells treated with the indicated doses of ATRA for 96 h (48 h + 48 h). (B – C) Cell viability assay on OVCAR-3 cells treated with the indicated concentration of NT20 and NT21 expressed as structured surfactant corresponding to ATRA-loaded niosomes containing 0.0015 mg/ml – 0.0030 mg/ml – 0.0060 mg/ml ATRA, respectively, for 96 h (48 h + 48 h). The results are expressed as the mean average deviation of %viable cells of three separate experiments and P-values were calculated using ordinary one-way ANOVA followed by Dunnett's post-hoc test. (D) Left panel - western blot analysis showing Pin1 endogenous protein levels in OVCAR-3 cells treated with NT20 123 μM and NT21 171 μM for 96 h (48 h + 48 h); **right panel** - graphs showing the relative quantification as determined by optical densitometry (OD). The results are expressed as the mean average deviations of three separate experiments and P-values were calculated using ordinary one-way ANOVA followed by Tukey's post-hoc test. (E) Left panel – western blot analysis showing Pin1 endogenous protein levels in OVCAR-3 cells treated with ATRA 0.0015 mg/ml, NT20A 0.0015 mg/ml, and NT21A 0.0015 mg/ml for 96 h (48 h + 48 h); **right panel** - graphs showing the relative quantification as determined by optical densitometry (OD). The results are expressed as the mean average deviations of three separate experiments and P-values were calculated using ordinary one-way ANOVA followed by Tukey's post-hoc test. (F) Cell survival of OVCAR-3 cells treated with ATRA 0.0015 mg/ml, NT20A 0.0015 mg/ml, and NT21A 0.0015 mg/ml for 96 h (48 h + 48 h). The results are expressed as the mean average deviation of %viable cells of three separate experiments and P-values were calculated using ordinary one-way ANOVA followed by Tukey's post-hoc test. In (A), (D), and (E) anti-Pin1 antibody was used to detect Pin1 protein levels, and anti-ß-actin or anti-vinculin antibodies were used as a loading control. In (B - E) values significance: ns = not significant $P > 0.05$, *$P \leq 0.05$, **$P \leq 0.001$, ***$P \leq 0.0001$.

9, panels E). Given that it has been demonstrated that Pin1 knock-down affects cell viability in ovarian cancer cell lines (Spena et al., 2018), we further investigated the short-term effects of ATRA-loaded niosomes: as shown in the panel F of all the Figs. 7-9, cell growth inhibition was significantly higher than that observed with free ATRA, which showed no effect. Therefore, we can infer that ATRA inhibits HGSOC cell growth mainly by inducing Pin1 degradation, as it has been demonstrated in hepatocellular carcinoma cell lines (Yang et al., 2018).

Taken together, these findings indicate that niosomes themselves have good biocompatibility and that ATRA-loaded niosomes offer improved ATRA efficacy even if ATRA payload seems apparently low (Table 2), thereby underscoring the potentiality of this promising nanotherapy for HGSOC-bearing patients.

Nevertheless, questions remain open on the reason why ATRA-loaded niosomes significantly enhance ATRA effects. More extensive studies will be carried out to understand how ATRA-loaded niosomes act on the cells by investigating in detail their cellular uptake. Specifically, we will investigate whether our pH-sensitive ATRA-loaded niosomes can mediate cytoplasm delivery through endocytosis and endo-lysosomal escape, consistently with our previous studies on unloaded niosomes (Carafa et al., 2006; Di Marzio et al., 2008). Furthermore, *in vivo* experiments will be carried out to provide further proof of concept for this promising nanotherapy.

4. Conclusions

The golden thread of the present multidisciplinary study was to assess whether the use of niosomes improves the pharmaceutical and therapeutic properties of ATRA.

Noteworthy, Tween 20 and Tween 21 niosomes appear to be a suitable carrier of ATRA because they showed good stability. The results are especially promising because the formulated niosomes showed an efficient and stable ATRA entrapment also in the presence of 50 % of human serum, thereby underscoring the potentiality of their *in vivo* use as nanocarriers. Furthermore, ATRA is released from niosomes with a controlled different release profile, depending on pH value. At pH 7.4 the release is slow, a crucial result if considering the low stability of free ATRA and its high systemic toxicity. At acidic pH the controlled release profile is more rapid, thus allowing the ATRA release in tumoral targeted sites.

Notably, the resulting ATRA-loaded niosomes are biocompatible and more effective than free ATRA on HGSOC cell lines, two key requirements for drug delivery system clinical experimentation.

Taken together, these findings might be crucial for translational applications from the bench to the bedside and may foster a novel effective therapy for HGSOC-bearing patients.

Funding

CRediT authorship contribution statement

Maria Valeria Giuli: Conceptualization, Data curation, Funding acquisition, Supervision, Validation, Writing – original draft, Writing – review & editing. **Patrizia Nadia Hanieh:** Conceptualization, Data Curation, Supervision, Validation, Writing - original draft, Writing - review & editing. **Jacopo Forte:** Formal analysis, Investigation. **Maria Gioia Fabiano:** Conceptualization, Data curation, Funding acquisition, Supervision, Validation, Writing – original draft, Writing – review & editing. **Angelica Mancusi:** Formal analysis, Investigation. **Bianca Natiello:** Formal analysis, Investigation. **Federica Rinaldi:** Data curation, Validation, Writing – original draft, Writing – review & editing. **Elena Del Favero:** Data curation, Formal analysis, Funding acquisition, Investigation, Writing – original draft. **Maria Grazia Ammendolia:** Conceptualization, Data curation, Funding acquisition, Supervision, Validation, Writing – original draft, Writing – review & editing. **Carlotta Marianecci:** Data curation, Validation, Writing – original draft, Writing – review & editing. **Saula Checquolo:** Conceptualization, Data curation, Funding acquisition, Supervision, Validation, Writing – original draft, Writing – review & editing. **Maria Carafa:** Conceptualization, Data curation, Funding acquisition, Supervision, Validation, Writing – original draft, Writing – review & editing.

Declaration of competing interest

The authors declare that they have no known competing financial interests or personal relationships that could have appeared to influence the work reported in this paper.

Data availability

Data will be made available on request.

Acknowledgements

Appendix A. Supplementary data

Supplementary data to this article can be found online at https://doi.org/10.1016/j.ijpharm.2023.123672.

References

Amale, F.R., Ferdowsian, S., Hajrasouliha, S., Kazempoor, R., Mirzaie, A., Dakkali, M.S., Akbarzadeh, I., Meybodi, S.M., Mirghafouri, M., 2021. Gold nanoparticles loaded into niosomes: A novel approach for enhanced antitumor activity against human ovarian cancer. Adv. Powder Technol. 32, 4711–4722.

Asadipour, E., Asgari, M., Mousavi, P., Piri-Gharaghie, T., Ghajari, G., Mirzaie, A., 2023. Nano-Biotechnology and Challenges of Drug Delivery System in Cancer Treatment Pathway. Chem. Biodivers. e202201072.

Bao, L., Kimzey, A., Sauter, G., Sowadski, J.M., Lu, K.P., Wang, D.-G., 2004. Prevalent overexpression of prolyl isomerase Pin1 in human cancers. Am. J. Pathol. 164, 1727–1737. https://doi.org/10.1016/S0002-9440(10)63731-5.

Bareford, L.M., Swaan, P.W., 2007. Endocytic mechanisms for targeted drug delivery. Adv. Drug Deliv. Rev. 59, 748–758. https://doi.org/10.1016/j.addr.2007.06.008.

Barenholz, Y.C., 2012. Doxil®—The first FDA-approved nano-drug: Lessons learned. J. Control. Release 160, 117–134. https://doi.org/10.1016/j.jconrel.2012.03.020.

Beesley, V.L., Green, A.C., Wyld, D.K., O'Rourke, P., Wockner, L.F., Defazio, A., Butow, P.N., Price, M.A., Horwood, K.R., Clavarino, A.M., 2014. Quality of life and treatment response among women with platinum-resistant versus platinum-sensitive ovarian cancer treated for progression: a prospective analysis. Gynecol. Oncol. 132, 130–136. https://doi.org/10.1016/j.ygyno.2013.10.004.

Brisaert, M., Gabriëls, M., Matthijs, V., Plaizier-Vercammen, J., 2001. Liposomes with tretinoin: a physical and chemical evaluation. J. Pharm. Biomed. Anal. 26, 909–917. https://doi.org/10.1016/s0731-7085(01)00502-7.

Carafa, M., Di Marzio, L., Marianecci, C., Cinque, B., Lucania, G., Kajiwara, K., Cifone, M., Santucci, E., 2006. Designing Novel pH-Sensitive Non-Phospholipid Vesicle: Characterization and Cell Interaction. European Journal of Pharmaceutical Sciences 28, 385–393. https://doi.org/10.1016/j.ejps.2006.04.009.

Carafa, M., Marianecci, C., Rinaldi, F., Santucci, E., Tampucci, S., Monti, D., 2009. Span® and Tween® neutral and pH-sensitive vesicles: Characterization and in vitro skin permeation. J. Liposome Res. 19, 332–340. https://doi.org/10.3109/08982100903014994.

Chlapek, P., Slavikova, V., Mazanek, P., Sterba, J., Veselska, R., 2018. Why differentiation therapy sometimes fails: molecular mechanisms of resistance to retinoids. Int. J. Mol. Sci. 19, 132. https://doi.org/10.3390/ijms19010132.

Coscia, F., Watters, K., Curtis, M., Eckert, M., Chiang, C., Tyanova, S., Montag, A., Lastra, R., Lengyel, E., Mann, M., 2016. Integrative proteomic profiling of ovarian cancer cell lines reveals precursor cell associated proteins and functional status. Nat. Commun. 7, 12645. https://doi.org/10.1038/ncomms12645.

Cuomo, F., Ceglie, S., Miguel, M., Lindman, B., Lopez, F., 2021. Oral delivery of all-trans retinoic acid mediated by liposome carriers. Colloids Surf. B Biointerfaces 201, 111655. https://doi.org/10.1016/j.colsurfb.2021.111655.

Daneshamouz, S., Tabakhian, M., Tavakoli, N., JAFARI, M., 2005. Influence of liposomes and niosomes on the in vitro permeation and skin retention of finasteride.

Di Marzio, L., Marianecci, C., Cinque, B., Nazzarri, M., Cimini, A., Cristiano, L., Cifone, M., Alhaique, F., Carafa, M., 2008. pH-sensitive non-phospholipid vesicle and macrophage-like cells: binding, uptake and endocytotic pathway. Biochimica et Biophysica Acta (BBA)-Biomembranes 1778, 2749-2756. DOI: 10.1016/j. bbamem.2008.07.029.

Di Marzio, L., Marianecci, C., Petrone, M., Rinaldi, F., Carafa, M., 2011. Novel pH-sensitive non-ionic surfactant vesicles: comparison between Tween 21 and Tween 20. Colloids Surf. B Biointerfaces 82, 18–24. https://doi.org/10.1016/j.colsurfb.2010.08.004.

Domcke, S., Sinha, R., Levine, D., Sander, C., Schultz, N., 2013. Evaluating cell lines as tumour models by comparison of genomic profiles. Nat Commun 4, 2126. https://doi.org/10.1038/ncomms3126.

Doucet, M., Cho, J., Alina, G., Bakker, J., Bouwman, W., Butler, P., Campbell, K., Gonzales, M., Heenan, R., Jackson, A., SasView version 4.2. 2. 2019.

Fattal, E., Couvreur, P., Dubernet, C., 2004. "Smart" delivery of antisense oligonucleotides by anionic pH-sensitive liposomes. Adv. Drug Deliv. Rev. 56, 931–946. https://doi.org/10.1016/j.addr.2003.10.037.

Franciosa, G., Diluvio, G., Del Gaudio, F., Giuli, M., Palermo, R., Grazioli, P., Campese, A., Talora, C., Bellavia, D., D'Amati, G., 2016. Prolyl-isomerase Pin1 controls Notch3 protein expression and regulates T-ALL progression. Oncogene 35, 4741–4751. https://doi.org/10.1038/onc.2016.5.

Giuli, M.V., Diluvio, G., Giuliani, E., Franciosa, G., Di Magno, L., Pignataro, M.G., Tottone, L., Nicoletti, C., Besharat, Z.M., Peruzzi, G., 2020a. Notch3 contributes to T-cell leukemia growth via regulation of the unfolded protein response. Oncogenesis 9, 93. https://doi.org/10.1038/s41389-020-00279-7.

Giuli, M.V., Hanieh, P.N., Giuliani, E., Rinaldi, F., Marianecci, C., Screpanti, I., Checquolo, S., Carafa, M., 2020b. Current trends in ATRA delivery for cancer therapy. Pharmaceutics 12, 707. https://doi.org/10.3390/pharmaceutics12080707.

Grace, V.M.B., Wilson, D.D., Guruvayoorappan, C., Danisha, J.P., Bonati, L., 2021. Liposome nano-formulation with cationic polar lipid DOTAP and cholesterol as a suitable pH-responsive carrier for molecular therapeutic drug (all-trans retinoic acid) delivery to lung cancer cells. IET Nanobiotechnol. 15, 380–390. https://doi.org/10.1049/nbt2.12028.

Haddadian, A., Robattorki, F.F., Dibah, H., Soheili, A., Ghanbarzadeh, E., Sartipnia, N., Hajrasouliha, S., Pasban, K., Andalibi, R., Ch, M.H., 2022. Niosomes-loaded selenium nanoparticles as a new approach for enhanced antibacterial, anti-biofilm, and anticancer activities. Sci. Rep. 12, 21938.

Hanieh, P.N., Consalvi, S., Forte, J., Cabiddu, G., De Logu, A., Poce, G., Rinaldi, F., Biava, M., Carafa, M., Marianecci, C., 2022. Nano-based drug delivery systems of potent mmpl3 inhibitors for tuberculosis treatment. Pharmaceutics 14, 610. https://doi.org/10.3390/pharmaceutics14030610.

Jones, M.-C., Ranger, M., Leroux, J.-C., 2003. pH-sensitive unimolecular polymeric micelles: synthesis of a novel drug carrier. Bioconjug. Chem. 14, 774–781. https://doi.org/10.1021/bc020041f.

Kano, K., Fendler, J.H., 1978. Pyranine as a sensitive pH probe for liposome interiors and surfaces. pH gradients across phospholipid vesicles. Biochimica Et Biophysica Acta (BBA)-Biomembranes 509, 289–299. https://doi.org/10.1016/0005-2736(78)90048-2.

Kazi, K.M., Mandal, A.S., Biswas, N., Guha, A., Chatterjee, S., Behera, M., Kuotsu, K., 2010. Niosome: a future of targeted drug delivery systems. J. Adv. Pharm. Technol. Res. 1, 374. https://doi.org/10.4103/0110-5558.76435.

Kobanenko, M.K., Tretiakova, D.S., Shchegravina, E.S., Antipova, N.V., Boldyrev, I.A., Fedorov, A.Y., Vodovozova, E.L., Onishchenko, N.R., 2022. Liposomal formulation of a PLA2-sensitive phospholipid–allocolchicinoid conjugate: Stability and activity studies in vitro. Int. J. Mol. Sci. 23, 1034. https://doi.org/10.3390/ijms23031034.

Kurnit, K.C., Fleming, G.F., Lengyel, E., 2021. Updates and new options in advanced epithelial ovarian cancer treatment. Obstet. Gynecol. 137, 108. https://doi.org/10.1097/AOG.0000000000004173.

Kuroki, L., Guntupalli, S.R., 2020. Treatment of epithelial ovarian cancer. BMJ 371. https://doi.org/10.1136/bmj.m3773.

Liou, Y.-C., Ryo, A., Huang, H.-K., Lu, P.-J., Bronson, R., Fujimori, F., Uchida, T., Hunter, T., Lu, K.P., 2002. Loss of Pin1 function in the mouse causes phenotypes resembling cyclin D1-null phenotypes. Proc. Natl. Acad. Sci. 99, 1335–1340. https://doi.org/10.1073/pnas.032404099.

Liu, D., Huang, L., 1989. Small, but not large, unilamellar liposomes composed of dioleoylphosphatidylethanolamine and oleic acid can be stabilized by human plasma. Biochemistry 28, 7700–7707. https://doi.org/10.1021/bi00445a027.

Lokman, N.A., Ho, R., Gunasegaran, K., Bonner, W.M., Oehler, M.K., Ricciardelli, C., 2019. Anti-tumour effects of all-trans retinoid acid on serous ovarian cancer. J. Exp. Clin. Cancer Res. 38, 1–12. https://doi.org/10.1186/s13046-018-1017-7.

Losi, L., Lauriola, A., Tazzioli, E., Gozzi, G., Scurani, L., D'Arca, D., Benhattar, J., 2019. Involvement of epigenetic modification of TERT promoter in response to all-trans retinoic acid in ovarian cancer cell lines. Journal of Ovarian Research 12, 1–10. https://doi.org/10.1186/s13048-019-0536-y.

Lu, Z., Hunter, T., 2014. Prolyl isomerase Pin1 in cancer. Cell Res. 24, 1033–1049. https://doi.org/10.1038/cr.2014.109.

Manconi, M., Sinico, C., Valenti, D., Loy, G., Fadda, A.M., 2002. Niosomes as carriers for tretinoin. I. Preparation and properties. Int. J. Pharm. 234, 237–248. https://doi.org/10.1016/s0378-5173(01)00971-1.

Marianecci, C., Di Marzio, L., Rinaldi, F., Celia, C., Paolino, D., Alhaique, F., Esposito, S., Carafa, M., 2014. Niosomes from 80s to present: the state of the art. Adv. Colloid Interface Sci. 205, 187–206. https://doi.org/10.1016/j.cis.2013.11.018.

Masetti, R., Biagi, C., Zama, D., Vendemini, F., Martoni, A., Morello, W., Gasperini, P., Pession, A., 2012. Retinoids in pediatric onco-hematology: the model of acute promyelocytic leukemia and neuroblastoma. Adv. Ther. 29, 747–762. https://doi.org/10.1007/s12325-012-0047-3.

Mirzaei-Parsa, M.J., Najafabadi, M.R.H., Haeri, A., Zahmatkeshan, M., Ebrahimi, S.A., Pazoki-Toroudi, H., Adel, M., 2020. Preparation, characterization, and evaluation of the anticancer activity of artemether-loaded nano-niosomes against breast cancer. Breast Cancer 27, 243–251. https://doi.org/10.1007/s12282-019-01014-w.

Moraru, C., Mincea, M., Menghiu, G., Ostafe, V., 2020. Understanding the factors influencing chitosan-based nanoparticles-protein corona interaction and drug delivery applications. Molecules 25, 4758. DOI: https://doi.org/10.3390%2Fmolecules25204758.

Muindi, J., Frankel, S.R., Miller Jr, W.H., Jakubowski, A., Scheinberg, D.A., Young, C.W., Dmitrovsky, E., Warrell Jr, R.P., 1992. Continuous treatment with all-transretinoic acid causes a progressive reduction in plasma drug concentrations: implications for relapse and retinoid "resistance" in patients with acute promyelocytic leukemia. Blood 79, 299–303. https://doi.org/10.1182/blood.V79.2.299.299.

Müller, R.H., Jacobs, C., Kayser, O., 2001. Nanosuspensions as particulate drug formulations in therapy: rationale for development and what we can expect for the future. Adv. Drug Deliv. Rev. 47, 3–19. https://doi.org/10.1016/s0169-409x(00)00118-6.

Na, K., Lee, K.H., Bae, Y.H., 2004. pH-sensitivity and pH-dependent interior structural change of self-assembled hydrogel nanoparticles of pullulan acetate/oligo-sulfonamide conjugate. J. Control. Release 97, 513–525. https://doi.org/10.1016/j.jconrel.2004.04.005.

Narvekar, M., Xue, H.Y., Wong, H.L., 2012. A novel hybrid delivery system: polymer-oil nanostructured carrier for controlled delivery of highly lipophilic drug all-trans-retinoic acid (ATRA). Int. J. Pharm. 436, 721–731. https://doi.org/10.1016/j.ijpharm.2012.07.042.

Nerli, G., Robla, S., Bartalesi, M., Luceri, C., D'Ambrosio, M., Csaba, N., Maestrelli, F., 2023. Chitosan coated niosomes for nose-to-brain delivery of clonazepam: formulation, stability and permeability studies. Carbohydrate Polymer Technologies and Applications 100332.

Ozpolat, B., Lopez-Berestein, G., Adamson, P., Fu, C., Williams, A.H., 2003. Pharmacokinetics of intravenously administered liposomal all-trans-retinoic acid (ATRA) and orally administered ATRA in healthy volunteers. J Pharm Pharm Sci 6, 292–301.

Pelullo, M., Nardozza, F., Zema, S., Quaranta, R., Nicoletti, C., Besharat, Z.M., Felli, M.P., Cerbelli, B., d'Amati, G., Palermo, R., 2019. Kras/ADAM17-dependent Jag1-ICD reverse signaling sustains colorectal cancer progression and chemoresistance. Cancer Res. 79, 5575–5586. https://doi.org/10.1158/0008-5472.CAN-19-0145.

Piri-Gharaghie, T., Beiranvand, S., Riahi, A., Shirin, N.J., Badmasti, F., Mirzaie, A., Elahianfar, Y., Ghahari, S., Ghahari, S., Pasban, K., 2022. Fabrication and characterization of thymol-loaded chitosan nanogels: improved antibacterial and anti-biofilm activities with negligible cytotoxicity. Chem. Biodivers. 19, e202100426.

Pourmoghadasiyan, B., Tavakkoli, F., Beram, F.M., Badmasti, F., Mirzaie, A., Kazempour, R., Rahimi, S., Larijani, S.F., Hejabi, F., Sedaghatnia, K., 2022. Nanosized paclitaxel-loaded niosomes: Formulation, in vitro cytotoxicity, and apoptosis gene expression in breast cancer cell lines. Mol. Biol. Rep. 49, 3597–3608.

Rahat, I., Imam, S.S., Rizwanullah, M., Alshehri, S., Asif, M., Kala, C., Taleuzzaman, M., 2021. Thymoquinone-entrapped chitosan-modified nanoparticles: formulation optimization to preclinical bioavailability assessments. Drug Deliv. 28, 973–984. https://doi.org/10.1080/10717544.2021.1927245.

Rinaldi, F., Hanieh, P.N., Marianecci, C., Carafa, M., 2015. DLS characterization of non-ionic surfactant vesicles for potential nose to brain application. Nanoscience and Nanometrology 1, 8–14. https://doi.org/10.11648/j.nsnm.20150101.12.

Rinaldi, F., Seguella, L., Gigli, S., Hanieh, P., Del Favero, E., Cantù, L., Pesce, M., Sarnelli, G., Marianecci, C., Esposito, G., 2019. inPentasomes: An innovative nose-to-brain pentamidine delivery blunts MPTP parkinsonism in mice. J. Control. Release 294, 17–26. https://doi.org/10.1016/j.jconrel.2018.12.007.

Rinaldi, F., Forte, J., Pontecorvi, G., Hanieh, P.N., Carè, A., Bellenghi, M., Tirelli, V., Ammendolia, M.G., Mattia, G., Marianecci, C., 2022. pH-responsive oleic acid based nanocarriers: Melanoma treatment strategies. Int. J. Pharm. 613, 121391 https://doi.org/10.1016/j.ijpharm.2021.121391.

Roux, E., Francis, M., Winnik, F.M., Leroux, J.-C., 2002. Polymer based pH-sensitive carriers as a means to improve the cytoplasmic delivery of drugs. Int. J. Pharm. 242, 25–36. https://doi.org/10.1016/s0378-5173(02)00183-7.

Russo Spena, C., De Stefano, L., Poli, G., Granchi, C., El Boustani, M., Ecca, F., Grassi, G., Grassi, M., Canzonieri, V., Giordano, A., 2019. Virtual screening identifies a PIN1 inhibitor with possible antiovarian cancer effects. J. Cell. Physiol. 234, 15708–15716. https://doi.org/10.1002/jcp.28224.

Santucci, E., Carafa, M., Coviello, T., Murtas, E., Riccieri, F.M., Alhaique, F., Modesti, A., Modica, A., 1996. Vesicles from polysorbate 20 and cholesterol: a simple preparation and characterization. STP Pharma Sciences 6, 29–32.

Schoellhammer, C.M., Blankschtein, D., Langer, R., 2014. Skin permeabilization for transdermal drug delivery: recent advances and future prospects. Expert Opin. Drug Deliv. 11, 393–407. https://doi.org/10.1517/17425247.2014.875528.

Senior, J., Gregoriadis, G., 1982. Stability of small unilamellar liposomes in serum and clearance from the circulation: the effect of the phospholipid and cholesterol components. Life Sci. 30, 2123–2136. https://doi.org/10.1016/0024-3205(82)90455-6.

Shadvar, P., Mirzaie, A., Yazdani, S., 2021. Fabrication and optimization of amoxicillin-loaded niosomes: an appropriate strategy to increase antimicrobial and anti-biofilm effects against multidrug-resistant Staphylococcus aureus strains. Drug Dev. Ind. Pharm. 47, 1568–1577.

Shinitzky, M., Barenholz, Y., 1978. Fluidity parameters of lipid regions determined by fluorescence polarization. Biochimica et Biophysica Acta (BBA)-Reviews on Biomembranes 515, 367–394. https://doi.org/10.1016/0304-4157(78)90010-2.

Simoes, S., Slepushkin, V., Düzgünes, N., de Lima, M.C.P., 2001. On the mechanisms of internalization and intracellular delivery mediated by pH-sensitive liposomes. Biochimica Et Biophysica Acta (BBA)-Biomembranes 1515, 23–37. https://doi.org/10.1016/s0005-2736(01)00389-3.

Song, M., Cui, M., Liu, K., 2022. Therapeutic strategies to overcome cisplatin resistance in ovarian cancer. Eur. J. Med. Chem. 232, 114205 https://doi.org/10.1016/j.ejmech.2022.114205.

Spena, C.R., De Stefano, L., Palazzolo, S., Salis, B., Granchi, C., Minutolo, F., Tuccinardi, T., Fratamico, R., Crotti, S., D'Aronco, S., 2018. Liposomal delivery of a Pin1 inhibitor complexed with cyclodextrins as new therapy for high-grade serous ovarian cancer. J. Control. Release 281, 1–10. https://doi.org/10.1016/j.jconrel.2018.04.055.

Szuts, E.Z., Harosi, F.I., 1991. Solubility of retinoids in water. Arch. Biochem. Biophys. 287, 297–304. https://doi.org/10.1016/0003-9861(91)90482-X.

Torre, L.A., Trabert, B., DeSantis, C.E., Miller, K.D., Samimi, G., Runowicz, C.D., Gaudet, M.M., Jemal, A., Siegel, R.L., 2018. Ovarian cancer statistics, 2018. CA: a cancer journal for clinicians 68, 284-296. DOI: 10.3322/caac.21456.

Trapasso, E., Cosco, D., Celia, C., Fresta, M., Paolino, D., 2009. Retinoids: new use by innovative drug-delivery systems. Expert Opin. Drug Deliv. 6, 465–483. https://doi.org/10.1517/17425240902832827.

Turro, N.J., Kuo, P.L., 1986. Pyrene excimer formations in micelles of nonionic detergents and of water-soluble polymers. Langmuir 2, 438–442. https://doi.org/10.1021/la00070a011.

Vasilescu, M., Angelescu, D.G., Bandula, R., Staikos, G., 2011. Microstructure of polyelectrolyte nanoaggregates studied by fluorescence probe method. J. Fluoresc. 21, 2085–2091. https://doi.org/10.1007/s10895-011-0907-2.

Wei, S., Kozono, S., Kats, L., Nechama, M., Li, W., Guarnerio, J., Luo, M., You, M.-H., Yao, Y., Kondo, A., 2015. Active Pin1 is a key target of all-trans retinoic acid in acute promyelocytic leukemia and breast cancer. Nat. Med. 21, 457–466. https://doi.org/10.1038/nm.3839.

Yang, D., Luo, W., Wang, J., Zheng, M., Liao, X.-H., Zhang, N., Lu, W., Wang, L., Chen, A.-Z., Wu, W.-G., 2018. A novel controlled release formulation of the Pin1 inhibitor ATRA to improve liver cancer therapy by simultaneously blocking multiple cancer pathways. J. Control. Release 269, 405–422. https://doi.org/10.1016/j.jconrel.2017.11.031.

Yasamineh, S., Yasamineh, P., Kalajahi, H.G., Gholizadeh, O., Yekanipour, Z., Afkhami, H., Eslami, M., Kheirkhah, A.H., Taghizadeh, M., Yazdani, Y., 2022. A state-of-the-art review on the recent advances of niosomes as a targeted drug delivery system. Int. J. Pharm. 624, 121878 https://doi.org/10.1016/j.ijpharm.2022.121878.

Yoshioka, T., Sternberg, B., Florence, A.T., 1994. Preparation and properties of vesicles (niosomes) of sorbitan monoesters (Span 20, 40, 60 and 80) and a sorbitan triester (Span 85). Int. J. Pharm. 105, 1–6. https://doi.org/10.1016/0378-5173(94)90228-3.

Yu, J.H., Im, C.Y., Min, S.-H., 2020. Function of PIN1 in cancer development and its inhibitors as cancer therapeutics. Front. Cell Dev. Biol. 8, 120. https://doi.org/10.3389/fcell.2020.00120.

Zhou, X.Z., Lu, K.P., 2016. The isomerase PIN1 controls numerous cancer-driving pathways and is a unique drug target. Nat. Rev. Cancer 16, 463–478. https://doi.org/10.1038/nrc.2016.49.